NATIONAL ADVISORY COMMITTEE FOR AERONAUTICS

TECHNICAL NOTE

No. 1277

TWO-DIMENSIONAL WIND-TUNNEL INVESTIGATION OF THE NACA 64_1-012 AIRFOIL EQUIPPED WITH TWO TYPES OF LEADING-EDGE FLAP

By Felicien F. Fullmer, Jr.

Langley Memorial Aeronautical Laboratory
Langley Field, Va.

Washington
May 1947

NATIONAL ADVISORY COMMITTEE FOR AERONAUTICS

TECHNICAL NOTE NO. 1277

TWO-DIMENSIONAL WIND-TUNNEL INVESTIGATION OF THE NACA 64_1-012 AIRFOIL EQUIPPED WITH TWO TYPES OF LEADING-EDGE FLAP

By Felicien F. Fullmer, Jr.

SUMMARY

An investigation was made in the Langley two-dimensional low-turbulence pressure tunnel to determine the characteristics of leading-edge flaps used as high-lift devices. The investigation, conducted at a Reynolds number of 6.0×10^6, included tests of two 10-percent-chord leading-edge flaps, one intended to slide forward along the upper surface and the other hinged near the leading edge on the lower surface of an NACA 64_1-012 airfoil, with and without a 20-percent-chord trailing-edge split flap. Data are given to show the section lift characteristics for a range of flap deflections and the pitching-moment characteristics and lift characteristics with leading-edge roughness for the optimum flap arrangements.

The results indicate that the maximum section lift-coefficient increments for the optimum upper- and lower-surface leading-edge flap arrangements on the plain airfoil were 0.43 and 0.12, respectively. The corresponding increments in the angle of attack for maximum section lift coefficients were 4.0° and 1.4°, respectively. When the airfoil was fitted with the 20-percent-chord trailing-edge split flap deflected 60°, the optimum upper- and lower-surface leading-edge flaps produced increments of 0.81 and 0.43, respectively. The corresponding increments in the angle of attack for the maximum section lift coefficients were 6.9° and 3.9°. The highest maximum section lift coefficient, 2.98 at an angle of attack of 16.2°, was obtained when the upper-surface leading-edge flap was used in combination with the trailing-edge split flap. The deflection of either type leading-edge flap resulted in a forward movement of the aerodynamic center at high angles of attack. The lower-surface leading-edge-flap installation was less sensitive to leading-edge roughness than the upper-surface leading-edge flap arrangement. With the trailing-edge flap, the maximum section lift coefficient for the upper-surface leading-edge flap in the rough condition, however, was about the same at the maximum lift coefficient obtained for the lower-surface leading-edge flap in the smooth condition.

INTRODUCTION

The problem of obtaining adequate maximum lift coefficients on highly swept wings for high-speed aircraft has brought to light a need for a more thorough investigation of auxiliary high-lift devices, such as leading-edge flaps, leading-edge slots, and drooped leading-edge airfoils. Recent reports of tests of conventional unswept wings (references 1 and 2) which were obtained from the D.V.L. in Germany indicated that one of these devices, the leading-edge flap, when used in combination with a conventional split flap, produced a substantial increase in the maximum lift coefficient accompanied by an increase in the angle of attack at which the maximum lift coefficient was obtained. The German investigations, however, were carried out at very low Reynolds numbers on airfoil sections having maximum lift coefficients of only about 0.72. The present brief investigation was conducted in the Langley two-dimensional low-turbulence pressure tunnel to determine the characteristics of a lower-surface leading-edge flap similar to the flap tested by the Germans but tested at a higher value of the Reynolds number (6.0×10^6) and also to investigate an improved type (upper surface) leading-edge flap. The investigation included tests of an upper- and lower-surface leading-edge flap on an NACA 6-series airfoil with and without a trailing-edge split flap.

SYMBOLS

α_o airfoil section angle of attack

c_l airfoil section lift coefficient (l/qc)

$c_{m_{c/4}}$ airfoil section pitching-moment coefficient about airfoil quarter-chord point (m/qc^2)

$\Delta\alpha_o$ increment of section angle of attack for maximum section lift coefficient due to leading-edge flap deflection

$c_{l_{max}}$ maximum section lift coefficient

$\Delta c_{l_{max}}$ increment in maximum section lift coefficient due to leading-edge flap deflection

$\delta_{f_{L.E.}}$ deflection of leading-edge flap, degrees (zero when flap lies along surface, hinge line forward of flap trailing edge)

$\delta_{f_{T.E.}}$ deflection of trailing-edge flap, degrees

c chord of plain airfoil

R Reynolds number

l lift per unit span

m moment per unit span

q dynamic pressure

MODEL

The model, which was constructed of laminated mahogany, had a chord of 24 inches and was built to correspond to the ordinates of the NACA 64$_1$-012 airfoil section. (See table I.) The 20-percent-chord trailing-edge split flap, set at a deflection of 60° and used for some of these tests, was simulated by a prismatic block of laminated mahogany attached to the lower surface of the model as shown in figure 1(a).

The lower-surface leading-edge flap was attached to the surface of the model at a point 2.25 percent of the chord back of the leading edge as shown by figures 1(a), 1(b), and 2. The 10-percent-chord flap was shaped to conform to the contour of the airfoil lower surface between the 2.25- and 11.47-percent airfoil chord stations and had a leading-edge radius equal to 0.78 percent of the airfoil chord.

The upper-surface flap (fig. 3(a)) was designed in an attempt to eliminate some of the more obvious faults of the lower-surface flap such as the serious discontinuity which occurs at the hinge point and the relatively small increase in area which was obtained with the flap in its optimum deflected position. For these reasons the upper-surface flap was designed to fair smoothly into the airfoil upper surface when the flap was fully deflected and at the same time to provide a relatively large increase in the area. Furthermore, the curvature of the upper surface is fairly large near the leading edge and this curvature decreases gradually with distance from the leading edge.

The upper-surface flap used for these tests simulated an extensible type of flap which, when retracted, was intended to form an integral portion of the airfoil leading edge and upper surface. The profile of the first 50 percent of this flap was

identical in contour to that of the plain airfoil from the leading edge to the 5-percent-chord station, and the remaining 50 percent of this 10-percent chord flap was of true circular-arc contour. The flap could thus be extended by sliding it along a circular-arc track. The radius used to describe this circular arc and the location of the center of curvature was chosen so that the arc conformed to the contour of the airfoil upper surface between the 1.75- and 5.00-percent-chord stations of the airfoil. Since the arc described by this radius formed a part of the original airfoil surface, the flap, when extended, faired smoothly into the airfoil upper surface to produce a highly cambered airfoil as shown in figures 3(a) and 3(b). The sketches of figure 4 show the ordinates, the relation of the flap to the model, and the method of measuring the effective 10-percent chord of the flap.

Both leading-edge flaps were constructed of $\frac{1}{16}$-inch sheet iron and were attached to the model by six brackets equally spaced across the 35.5-inch span of the model. The various deflections of the lower-surface flap were obtained by the installation of a new set of brackets for each deflection. The deflection of the lower-surface leading-edge flap was measured in a counterclockwise direction (fig. 2) from its retracted position. The 153° deflection for the upper-surface leading-edge flap as shown in figure 4 was given for the purpose of comparison with the flap deflections indicated in figure 2. The retracted positions of the flaps are shown by dotted lines in figures 2 and 4.

The leading-edge roughness used for the tests of the plain airfoil and the airfoil leading-edge flap configurations consisted of 0.01-inch carborundum grains shellacked to the airfoil upper and lower surfaces for a distance equal to 8 percent of the chord as measured from the intersection of the chord line and airfoil leading-edge radius. The roughness used for the test of the leading-edge flap arrangements consisted of similar size carborundum grains shellacked to the flap leading edge and to the forward 80 percent of the flap upper surface (fig. 3(b)).

TESTS

The lift characteristics were obtained for the model with each of the leading-edge flaps alone and in combination with the trailing-edge split flap deflected 60°. The pitching-moment characteristics for the model in a smooth condition and the lift characteristics for the model in a rough condition were obtained only for the more favorable flap settings of the various airfoil flap configurations. All tests were made at an absolute tank pressure of 59 pounds per

square inch and a dynamic pressure of approximately 70 pounds per square foot which correspond to a Reynolds number of 6.0×10^6 and a Mach number of 0.11.

Test Methods and Tunnel Corrections

The lift characteristics of airfoils tested in the Langley two-dimensional low-turbulence pressure tunnel are obtained by integrating, over a finite distance, the pressure distribution imposed by the model on the floor and ceiling of the tunnel. Because only about 93 percent of the actual lift is transferred to the floor and ceiling of the tunnel in the finite distance covered by the lift orifices, correction factors, obtained theoretically, were applied to the integrated pressure-distribution data to obtain the total lift.

Corrections for the wind-tunnel-wall effects were made by the following equations, where the primed symbols represent the quantities measured in the tunnel:

$$\alpha_o = 1.015\alpha_o'$$

$$c_l = 0.978c_l'$$

$$c_{m_{c/4}} = 0.993c_{m_{c/4}}'$$

A correction has also been applied to the data presented herein for the blocking effect at angles of attack near maximum lift. This correction for the blocking effect reduces the maximum lift coefficient measured in the tunnel by approximately 1.5 percent. Previous comparisons of the lift coefficients obtained from the measurement of the pressure reaction on the floor and ceiling of the tunnel were in close agreement with those obtained from airfoil pressure distributions and force tests. The probable error in individual test points as determined from check tests, consideration of the sensitivity of the measuring instruments, and the departure of points from the faired curves is estimated to be within the following limits:

Over the linear portion of the lift curve:

c_l	± 0.005
$c_{m_{c/4}}$	± 0.002
α_o	$\pm 0.1^\circ$

Near maximum lift coefficient:

c_l	± 0.020
$c_{m_{c/4}}$	± 0.010
α_o	$\pm 0.1^\circ$

RESULTS AND DISCUSSION

The lift characteristics obtained from tests of the various airfoil flap configurations are presented in figures 5 to 7. The pitching-moment characteristics of the plain airfoil, of the airfoil-trailing-edge flap model, and of the optimum airfoil-leading-edge-flap arrangements tested are presented in figure 8. The effect of leading-edge roughness on the lift characteristics of both the plain airfoil and the airfoil with the trailing-edge flap is shown in figure 9; similar data for the best airfoil-leading-edge-flap arrangements tested are presented in figure 10. The variation of the increments of maximum section lift coefficient $\Delta c_{l_{max}}$ and of section angle of attack for maximum section lift coefficient $\Delta\alpha_o$ with leading-edge flap deflection is presented in figure 11.

Lift Characteristics

The data presented in figures 5 to 7 show that the best arrangements of leading-edge flaps of the type tested increased the maximum section lift coefficient and also the section angle of attack at which the maximum lift coefficient occurs. The maximum section lift coefficients, the angles of attack at which the maximum section lift coefficient occurred, and the increments which were obtained for the various optimum configurations are summarized in the following table:

Model configuration	$c_{l_{max}}$	α_o (deg)	$\Delta c_{l_{max}}$	$\Delta\alpha_o$ (deg)	$\delta_{f_{L.E.}}$ (deg)	$\delta_{f_{T.E.}}$ (deg)
Airfoil alone	1.42	14.3	------	-----	------	------
Airfoil and lower-surface leading-edge flap	1.54	15.7	0.12	1.4	120	------
Airfoil and upper-surface leading-edge flap	1.85	18.3	.43	4.0	153	------
Airfoil and trailing-edge flap alone	2.17	9.3	------	-----	------	60
Airfoil trailing-edge flap and lower-surface leading-edge flap	2.60	13.2	.43	3.9	112	60
Airfoil trailing-edge flap and upper-surface leading-edge flap	2.98	16.2	.81	6.9	153	60

The leading-edge flap is believed to produce these increases in $c_{l_{max}}$ and in the angle of attack for $c_{l_{max}}$ by reducing the magnitude of the pressure peaks and the magnitude of the adverse pressure gradient usually associated with the flow conditions near maximum lift of the plain airfoil section. At the optimum deflection, the flap is so alined with the flow approaching the leading edge that a substantial amount of lift is carried by the flap without the presence of excessive pressure peaks. Some increase in lift is, of course, also associated with the effective increase in area caused by flap deflection. At flap deflections less than the optimum, the flow over the rear portion of the airfoil becomes separated before the angle of attack is high enough for the load on the flap to contribute substantially to the lift. At flap deflections greater than the optimum, large pressure peaks form at the leading edge of the flap at low angles of attack.

The effect of the leading-edge flap at angles of attack well below those for maximum lift is to act as a spoiler on the lower surface of the airfoil and thus to cause large reductions in lift. As the angle of attack is increased and the flow becomes better alined with the flap, the spoiler action of the flap decreases and the lift becomes equal to that of the plain airfoil at some moderate angle of attack. The slope of the lift curve is therefore much higher at low angles of attack for the flapped section than for the plain airfoil.

The preceding discussion is also applicable to the case of the airfoil leading-edge flap combination when fitted with a trailing-edge high-lift device. For this condition, the optimum leading-edge flap deflection is expected to be somewhat less than for the plain airfoil, because of the greater inclination of the flow to the airfoil chord at the leading edge.

Lower-surface flap.- An examination of the section lift characteristics presented in figure 5 shows that the lower-surface leading-edge flap, when used in conjunction with the plain airfoil, produced a maximum section lift coefficient of 1.54 at an angle of attack of 15.7° ($\delta_{f_{L.E.}} = 120°$), which correspond, as shown in figure 11, to increments $\Delta c_{l_{max}} = 0.12$ and $\Delta\alpha_o = 1.4°$ above the values obtainable with the plain airfoil. When this leading-edge flap was used in combination with the airfoil and split trailing-edge flap (fig. 6) the maximum section lift coefficient was increased to a value of 2.60 at an angle of attack of 13.2° ($\delta_{f_{L.E.}} = 112°$), which corresponded to increments $\Delta c_{l_{max}} = 0.43$ and $\Delta\alpha_o = 3.9°$ over and above that obtained with the conventional

airfoil and trailing-edge flap arrangement. German data (reference 1) indicated that an increment in maximum lift coefficient of 0.31 was obtained with a similar arrangement of leading-edge and trailing-edge flaps on an airfoil of the same thickness. It is apparent, however, from figures 5 and 6 that a leading-edge flap of this type is somewhat sensitive to changes in flap deflection for the reasons given in the previous general discussion of both types of leading-edge flaps. A comparison of the data presented in figures 5 and 6 and the increments obtained indicates that the presence of the split trailing-edge flap altered the flow characteristics in such a manner as to increase the effectiveness of the leading-edge flap at deflections as low as 103°. The cross plot (fig. 10) shows that the presence of the trailing-edge flap, as previously mentioned, had a pronounced effect on the deflection at which the best maximum lift coefficient increment was obtained. For example, the optimum deflection for the leading-edge flap when used alone was 120°, but when used in conjunction with the trailing-edge flap, the optimum deflection was 112°.

Upper-surface flap.- An examination of the section lift characteristics presented in figure 7 shows that this upper-surface leading-edge flap, when used in conjunction with the plain airfoil, produced a maximum section lift coefficient of 1.85 at an angle of attack of 18.3°. These values corresponded to an increment $\Delta c_{l_{max}} = 0.43$ and an increment $\Delta\alpha_o = 4.0°$ above the values obtainable with the plain airfoil. The same figure shows that the use of this leading-edge flap in conjunction with the airfoil and split trailing-edge flap produced a maximum lift coefficient of 2.98 at an angle of attack of 16.2°, which corresponded to increments $\Delta c_{l_{max}} = 0.81$ and $\Delta\alpha_o = 6.9°$ above that obtained for the airfoil and split trailing-edge flap arrangement. The data presented in figure 7 show that at low angles of attack this flap also produces decrements in the section lift coefficients. The rapid decrease in the magnitude of this decrement in lift coefficient shows, however, that the spoiler action is somewhat less severe for this flap than it is for the lower-surface leading-edge type of flap.

The results given in figure 11 indicate that the increments $\Delta c_{l_{max}}$ and $\Delta\alpha_o$ were considerably greater for the upper-surface leading-edge flap. This can be attributed to the slightly greater projected area and smooth contour of the upper-surface leading-edge flap.

Pitching-Moment Characteristics

A comparison of the pitching-moment data obtained for the plain airfoil and the airfoil trailing-edge flap arrangement with data obtained for the same arrangements equipped with the lower- or upper-surface leading-edge flaps (fig. 8) shows that the addition of either flap caused the moment coefficients to increase negatively with increasing lift coefficients until the angle of attack was approximately high enough for the flap to cease acting as a spoiler. As the lift coefficient is increased beyond this point, the moment coefficients increase positively in a manner corresponding to a forward position of aerodynamic center with respect to the quarter-chord point of the original model. Such a forward position of the aerodynamic center is consistent with the fact that area has been added ahead of the leading edge of the plain airfoil. The forward shift in the position of the aerodynamic center was slightly greater for the upper-surface flap installation than for the lower-surface flap installation. The results show that increments in pitching-moment coefficient which were obtained from the addition of either of the leading-edge flaps are relatively small in comparison with the increment resulting from deflection of the conventional split trailing-edge flap.

Effects of Leading-Edge Roughness

The decrements in the maximum section lift coefficient caused by the addition of leading-edge roughness were about 0.4 for the upper-surface leading-edge flap when used alone or when used in combination with the trailing-edge split flap. (See fig. 10(b).) These decrements are of the same order of magnitude as those obtained for the plain airfoil and the airfoil trailing-edge split-flap model as shown in figure 9. The corresponding decrements in the maximum section lift coefficients for the lower-surface leading-edge flap (fig. 10(a)), with leading-edge roughness, was approximately 0.1 without the trailing-edge flap, and approximately 0.2 with the 20-percent-chord trailing-edge split flap. The decrements caused by the addition of roughness to the leading edge of the lower-surface leading-edge flap are relatively low because the flow over the airfoil upper surface for this configuration is already seriously disturbed by the projecting leading edge of the normal airfoil. A comparison of the lift characteristics of both leading-edge flap arrangements (without trailing-edge flap) in a rough condition with those for the plain airfoil in a smooth condition shows that the maximum section lift coefficients are approximately of the same order of magnitude. With the trailing-edge split flap deflected 60°, however, the maximum section lift coefficient for the upper-surface leading-edge flap with roughness

at the leading edge is about the same as that for the lower-surface leading-edge flap configuration in the smooth condition and considerably higher than that for the conventional airfoil-trailing-edge flap in the same smooth condition.

CONCLUSIONS

This investigation, conducted at a Reynolds number of 6.0×10^6, was made to determine the lift and pitching-moment characteristics of two 10-percent-chord leading-edge flaps used as high-lift devices on an NACA 64_1-012 airfoil with and without a 20-percent-chord trailing-edge split flap deflected 60°. The upper-surface leading-edge flap was designed to slide forward and to fair smoothly into the airfoil contour, whereas the lower-surface leading-edge flap was hinged at the 2.25-percent-chord station. The results indicate the following conclusions:

1. The maximum section lift coefficient increments for the optimum upper- and lower-surface leading-edge flap arrangements on the plain airfoil were 0.43 and 0.12, respectively. The corresponding increments in the angle of attack for maximum section lift coefficients were 4.0° and 1.4°, respectively.

2. When the airfoil was fitted with the 20-percent-chord trailing-edge split flap, the optimum upper- and lower-surface leading-edge flap deflections produced increments of 0.81 and 0.43, respectively. The corresponding increments in the angle of attack for the maximum section lift coefficients were 6.9° and 3.9°.

3. The highest maximum section lift coefficient, 2.98 at an angle of attack of 16.2°, was obtained when the upper-surface leading-edge flap was used in combination with the trailing-edge split flap.

4. The deflection of either type leading-edge flap resulted in a forward movement of the aerodynamic center at high angles of attack.

5. The lower-surface leading-edge flap installation was less sensitive to leading-edge roughness than the upper-surface leading-edge flap arrangement. With the trailing-edge flap, the maximum section lift coefficient for the upper-surface leading-

edge flap in the rough condition, however, was about the same as the maximum lift coefficient obtained for the lower-surface flap in the smooth condition.

Langley Memorial Aeronautical Laboratory
National Advisory Committee for Aeronautics
Langley Field, Va., January 21, 1947

REFERENCES

1. Koster, H.: Messungen am Profil $NACA_E$ 0 00 12 - 0,55 45 mit Spreiz- und Nasenspreizklappe. UM Nr. 1317, Deutsche Luftfahrtforschung (Berlin-Adlershof), 1944.

2. Kruger, W.: Systematische Windkanalmessungen an einem Laminarflugel mit Nasenklappe. Forschungsbericht Nr. 1948, Deutsche Luftfahrtforschung (Gottingen), 1944.

TABLE I

ORDINATES FOR NACA 64_1-012 AIRFOIL

[Stations and ordinates given in percent of airfoil chord]

Upper surface		Lower surface	
Station	Ordinate	Station	Ordinate
0	0	0	0
.5	.978	.5	-.978
.75	1.179	.75	-1.179
1.25	1.490	1.25	-1.490
1.75	1.730	1.75	-1.730
2.5	2.035	2.5	-2.035
5.0	2.810	5.0	-2.810
7.5	3.394	7.5	-3.394
10.0	3.871	10.0	-3.871
15.0	4.620	15.0	-4.620
20.0	5.173	20.0	-5.173
25.0	5.576	25.0	-5.576
30.0	5.844	30.0	-5.844
35.0	5.978	35.0	-5.978
40.0	5.981	40.0	-5.981
45.0	5.798	45.0	-5.798
50.0	5.480	50.0	-5.480
55.0	5.056	55.0	-5.056
60.0	4.548	60.0	-4.548
65.0	3.974	65.0	-3.974
70.0	3.350	70.0	-3.350
75.0	2.695	75.0	-2.695
80.0	2.029	80.0	-2.029
85.0	1.382	85.0	-1.382
90.0	.786	90.0	-.786
95.0	.288	95.0	-.288
100	0	100	0
L. E. radius: 1.040			

NATIONAL ADVISORY
COMMITTEE FOR AERONAUTICS

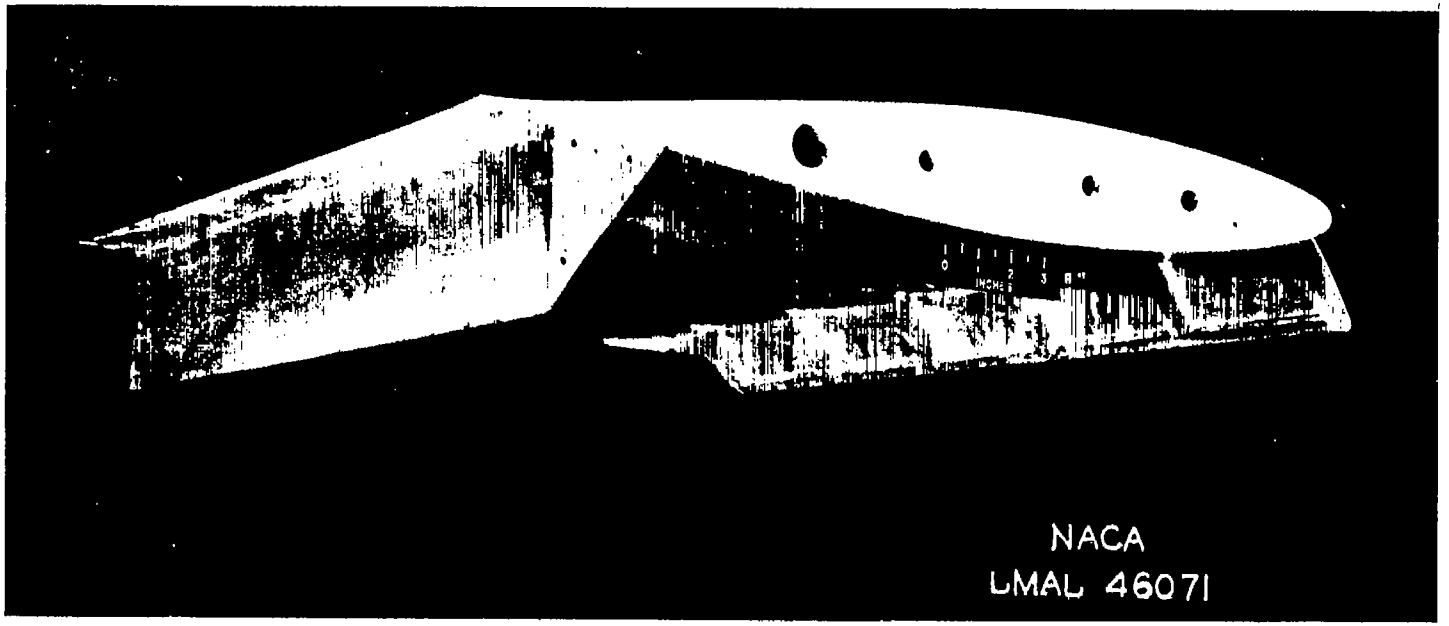

(a) Three-quarter rear view of model showing the installation of the leading- and trailing-edge flaps.

Figure 1.- Photographs of the NACA 64_1-012 airfoil section and the 0.10c lower-surface leading-edge flap alone and in combination with the 0.20c trailing-edge split flap.

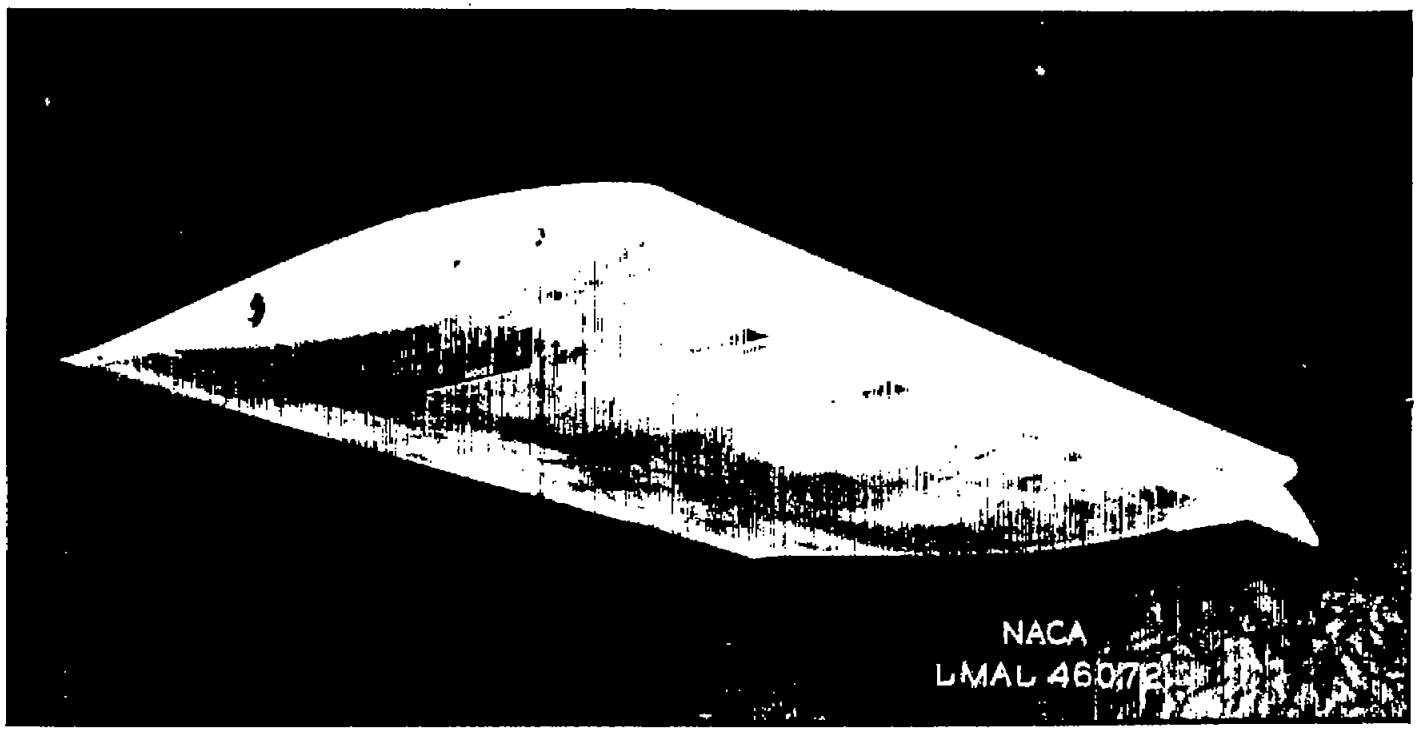

(b) Three-quarter front view of the model showing the contour of the lower-surface leading-edge flap.

Figure 1.- Concluded.

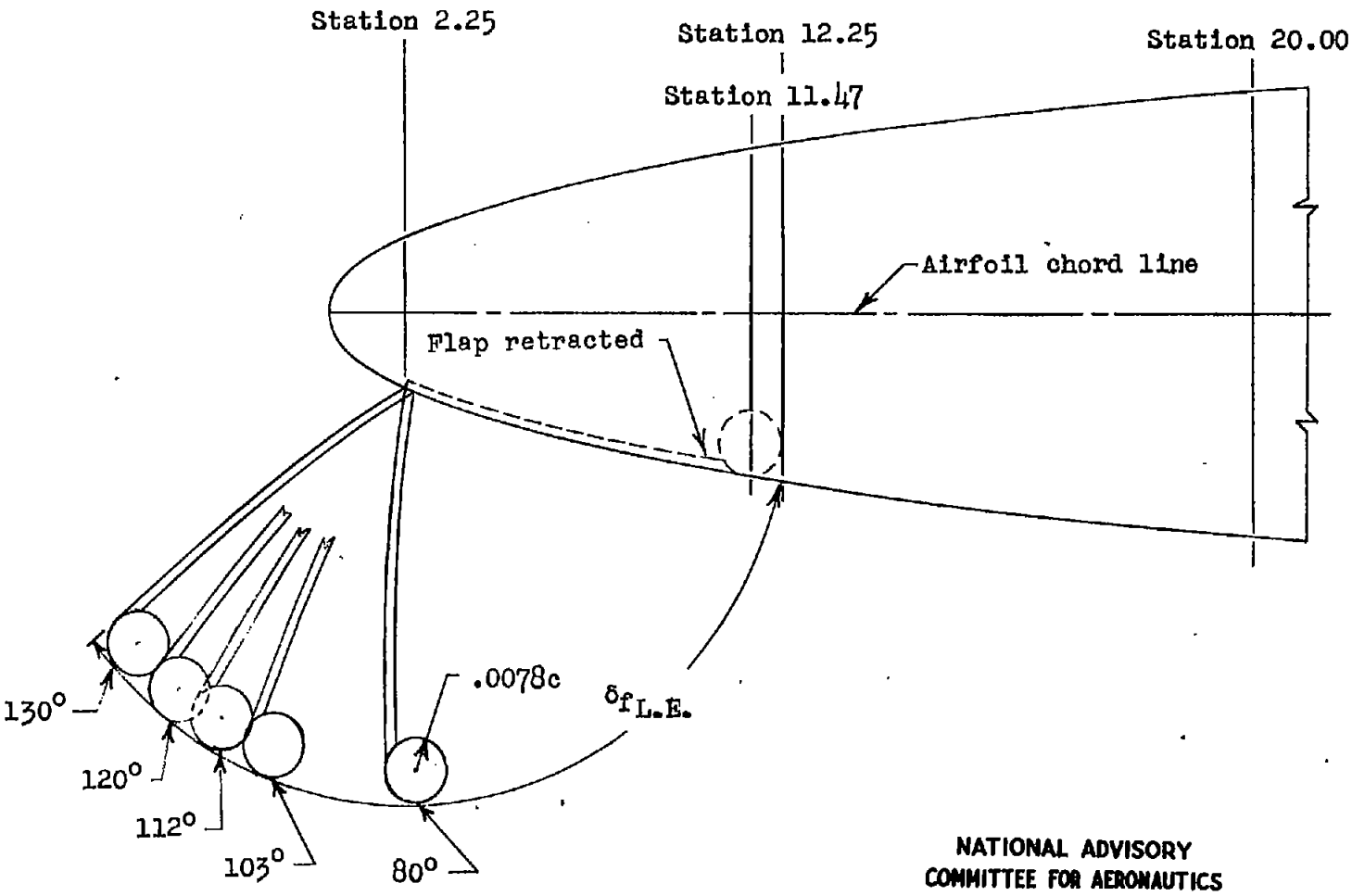

Figure 2.- Sketch showing the lower-surface leading-edge flap arrangement on the NACA 64_1-012 airfoil section.

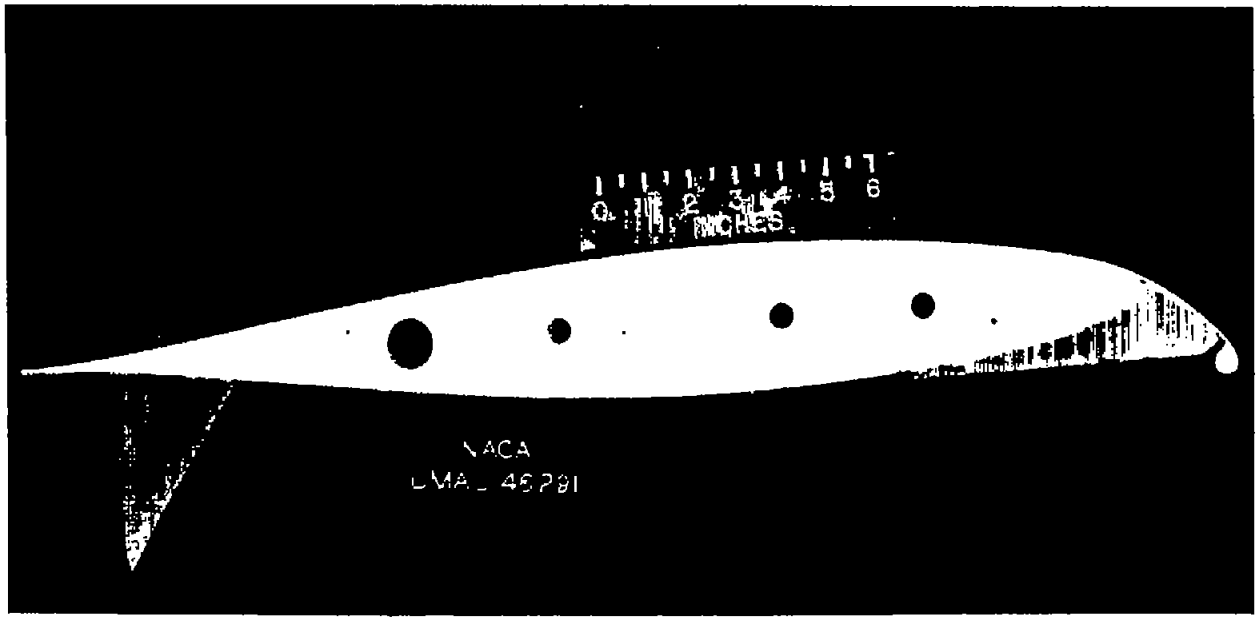

(a) Side view of model showing installation of upper-surface leading-edge flap and lower-surface trailing-edge flap.

Figure 3.- Photographs of the NACA 64_1-012 airfoil section and the 0.10c upper-surface leading-edge flap alone and in combination with the 0.20c trailing-edge split flap.

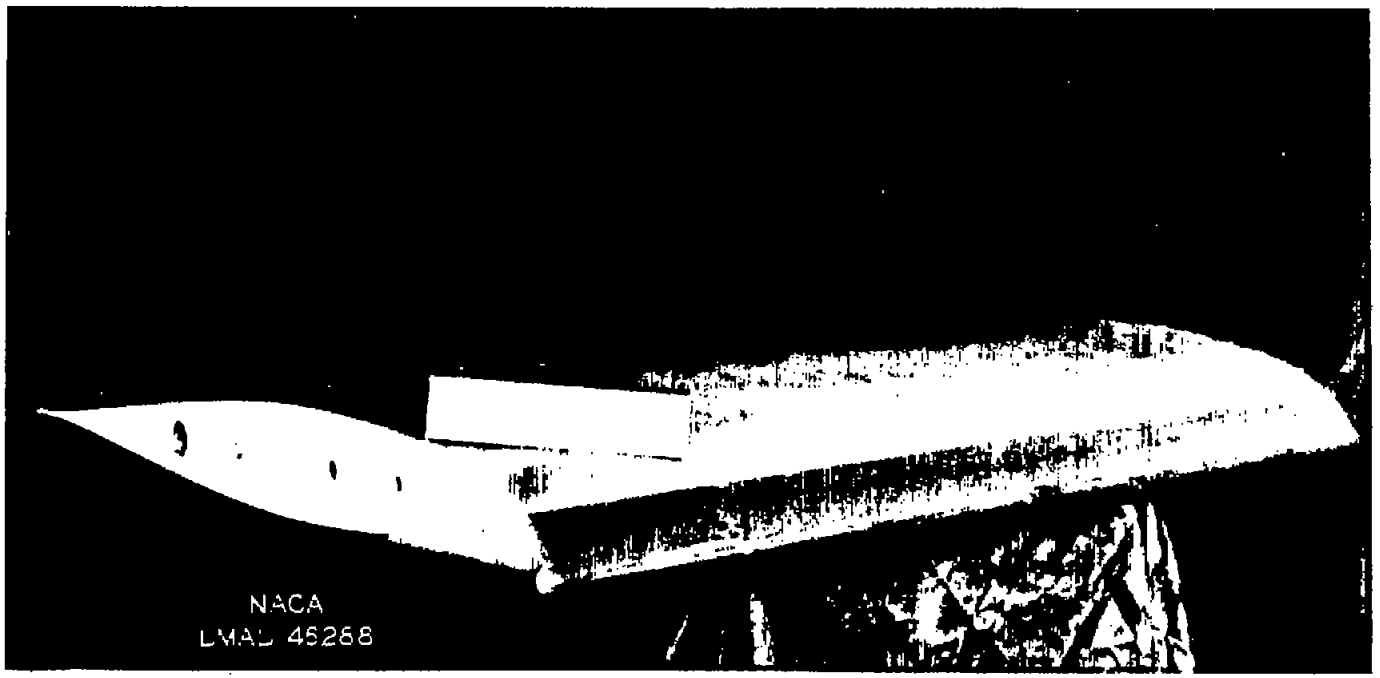

(b) Three-quarter front view of model showing the leading-edge roughness applied to upper-surface leading-edge flap.

Figure 3.- Concluded.

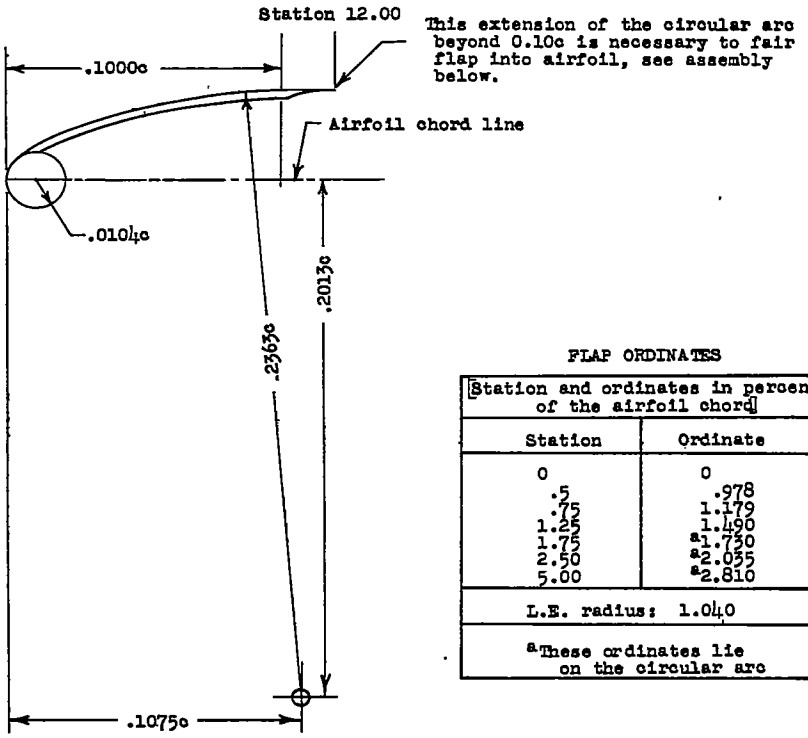

FLAP ORDINATES

Station and ordinates in percent of the airfoil chord

Station	Ordinate
0	0
.5	.978
.75	1.179
1.25	1.490
1.75	[a]1.730
2.50	[a]2.035
5.00	[a]2.810

L.E. radius: 1.040

[a]These ordinates lie on the circular arc

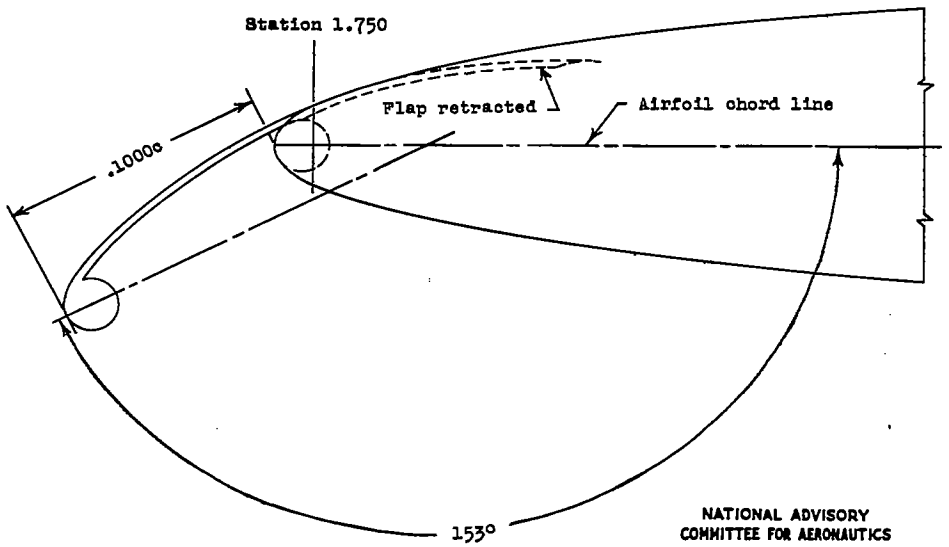

Figure 4.- Sketch showing the upper-surface leading-edge flap, flap ordinates, and the arrangements of the flap on the NACA 64_1-012 airfoil section.

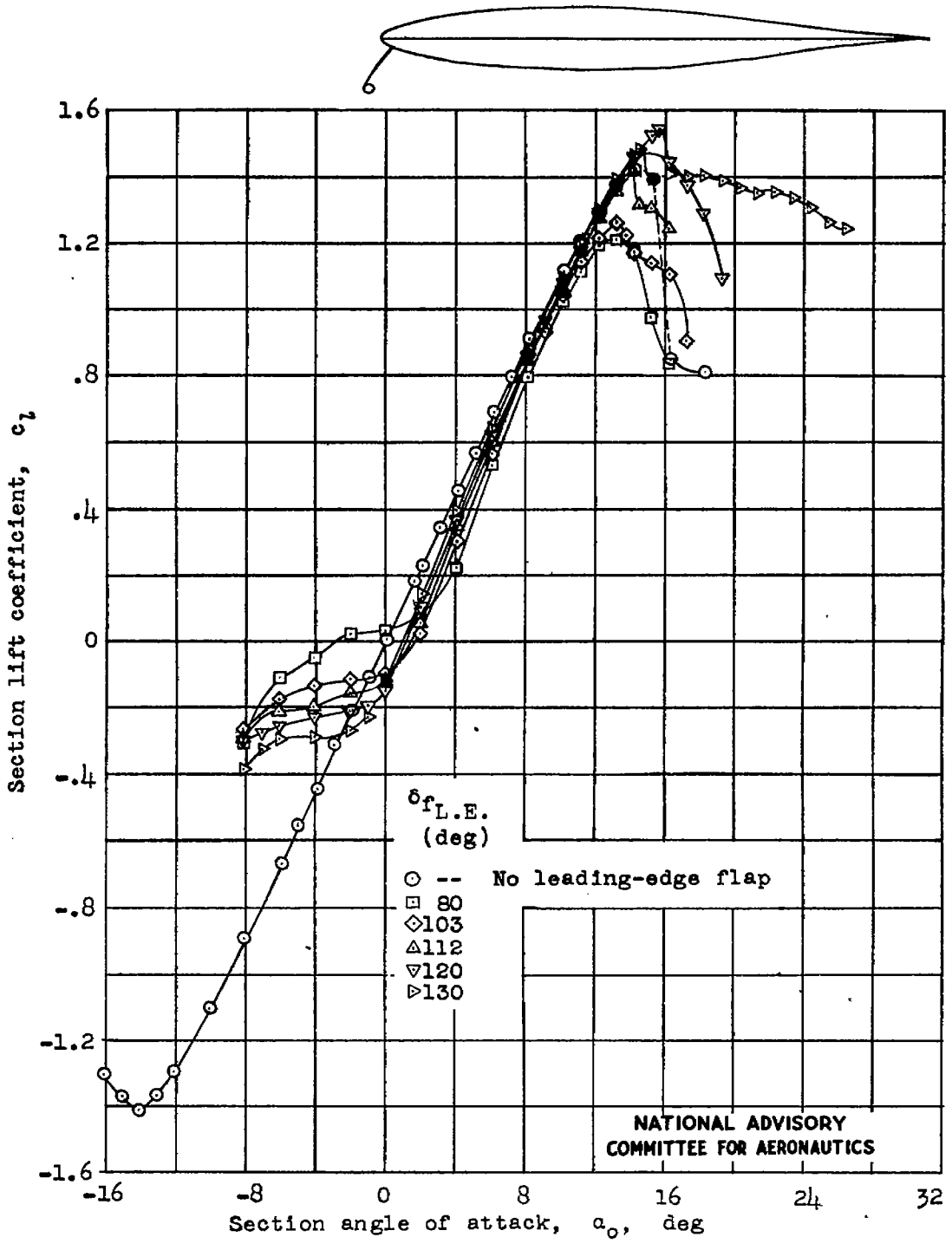

Figure 5.- Section lift characteristics for the NACA 64_1-012 airfoil section equipped with a 0.10c lower-surface leading-edge flap. $R = 6.0 \times 10^6$.

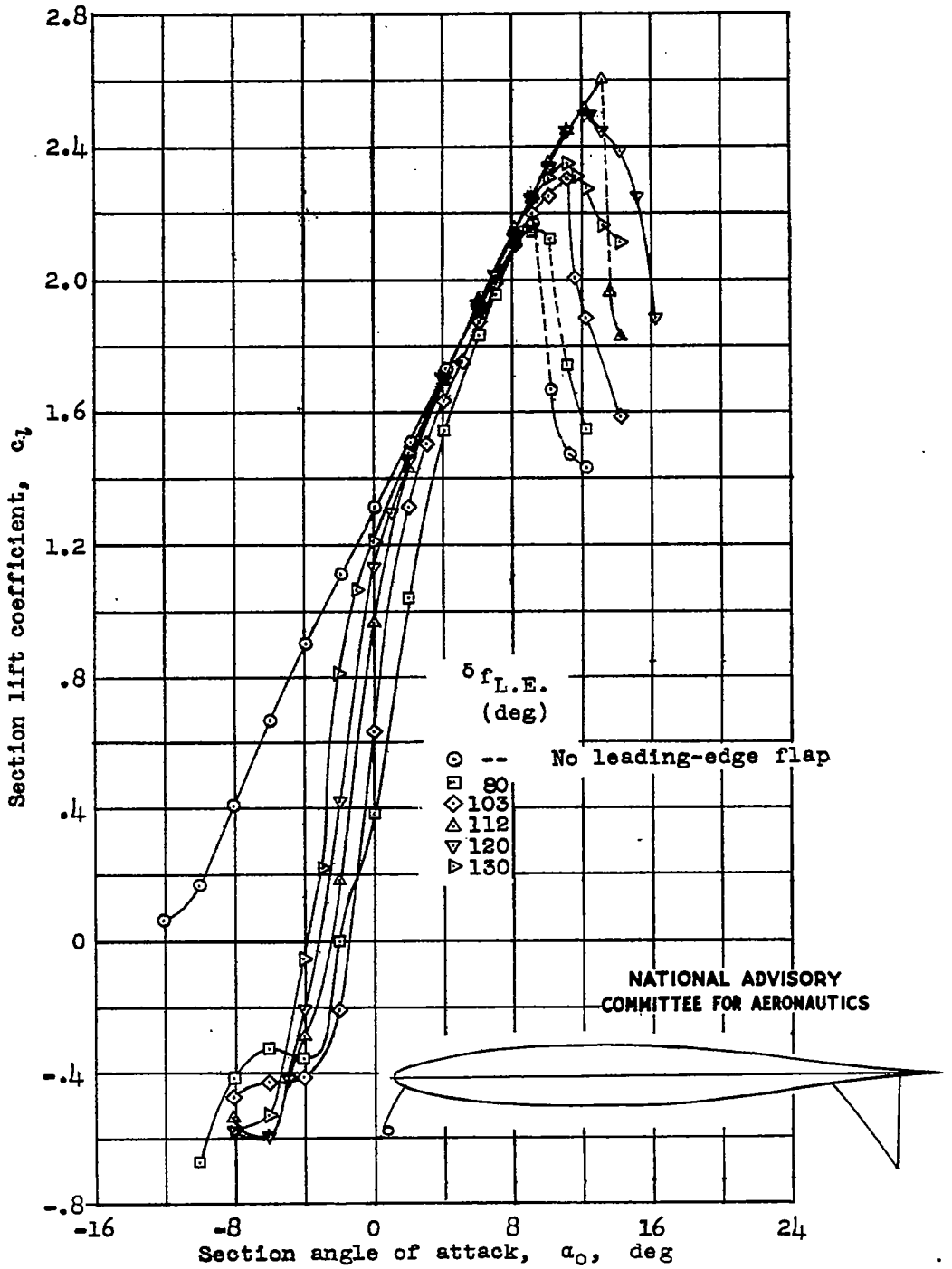

Figure 6.- Section lift characteristics for the NACA 64_1-012 airfoil section equipped with a 0.10c lower-surface leading-edge flap and a 0.20c trailing-edge split flap. $R = 6.0 \times 10^6$, $\delta_{f_{T.E.}} = 60°$.

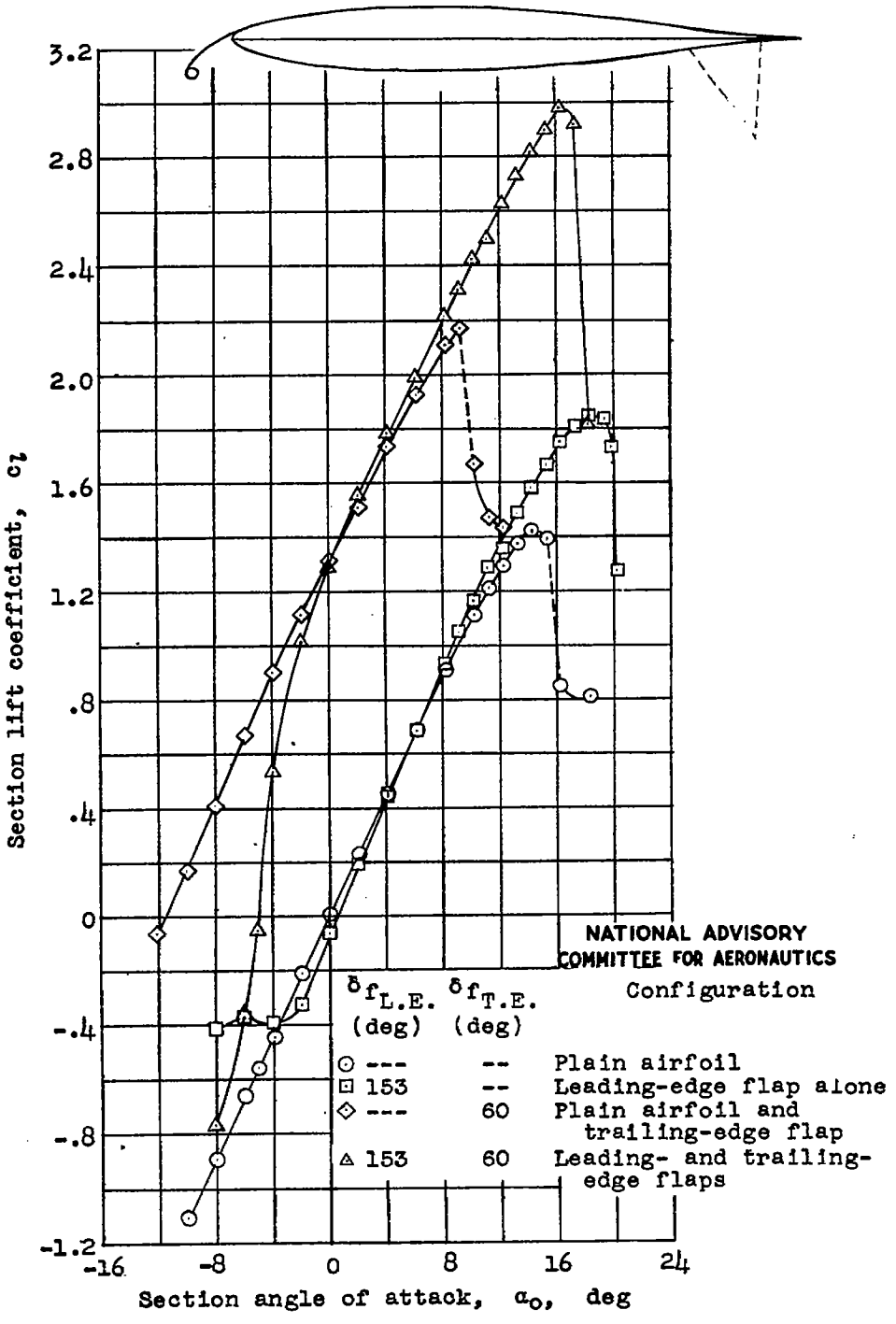

Figure 7.- Section lift characteristics for the NACA 64_1-012 airfoil section equipped with a 0.10c upper-surface leading-edge flap alone, and in combination with a 0.20c trailing-edge split flap. $R = 6.0 \times 10^6$.

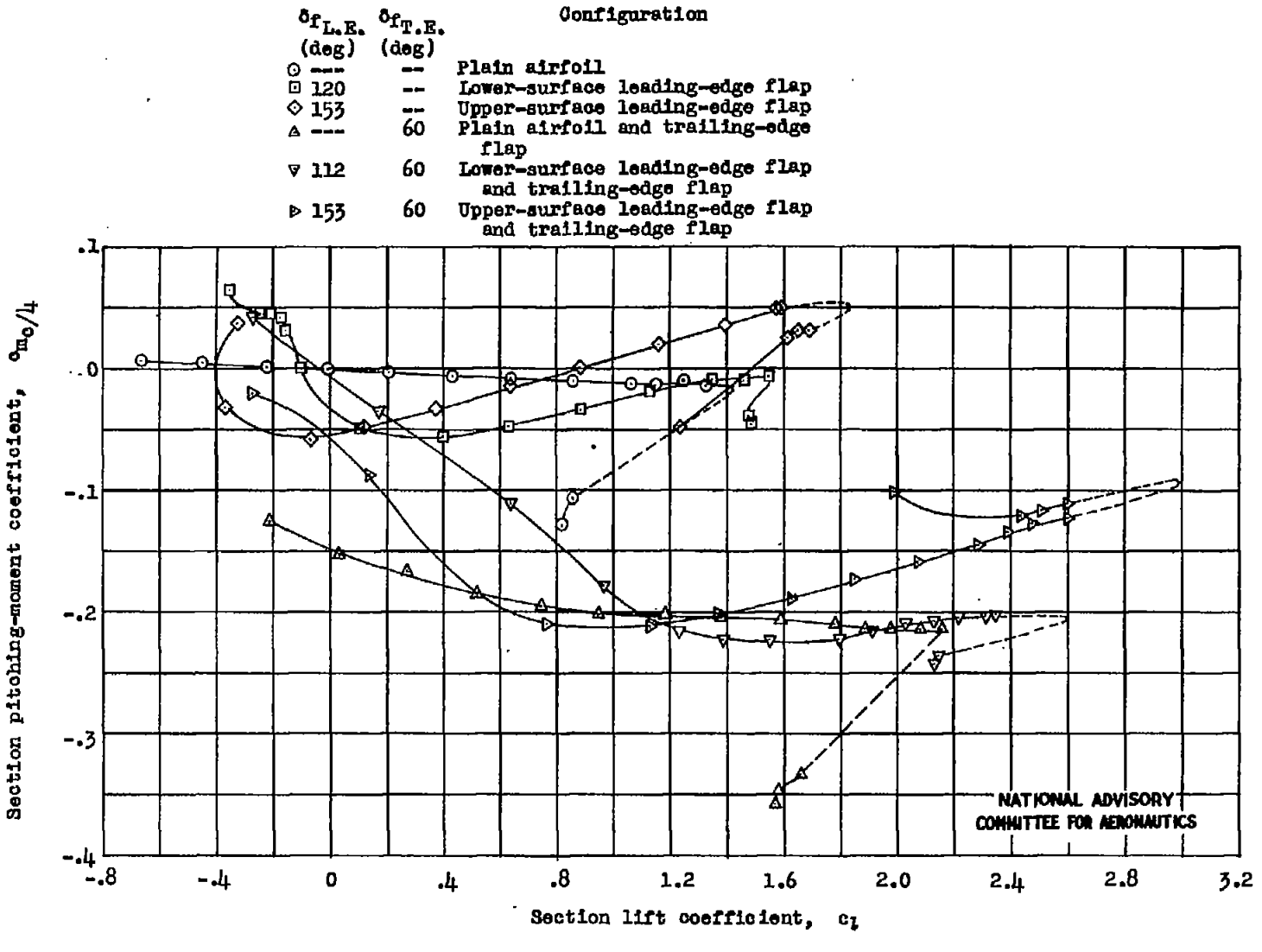

Figure 8.- Section pitching-moment characteristics for the NACA 64_1-012 airfoil with and without the optimum leading-edge and trailing-edge flaps. $R = 6.0 \times 10^6$.

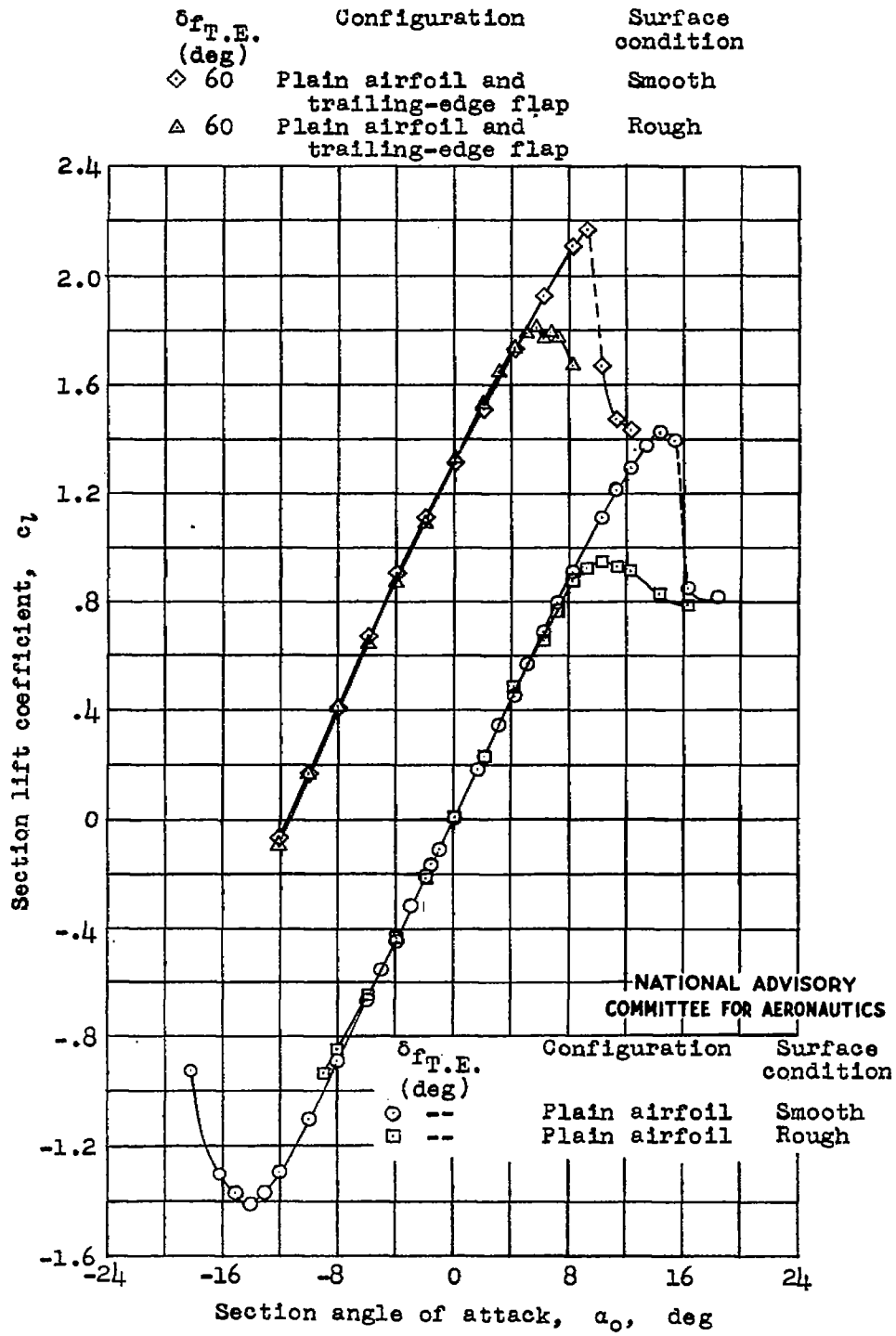

Figure 9.- The effect of leading-edge roughness on the section lift characteristics of the NACA 64_1-012 airfoil with and without a trailing-edge split flap. $R = 6.0 \times 10^6$.

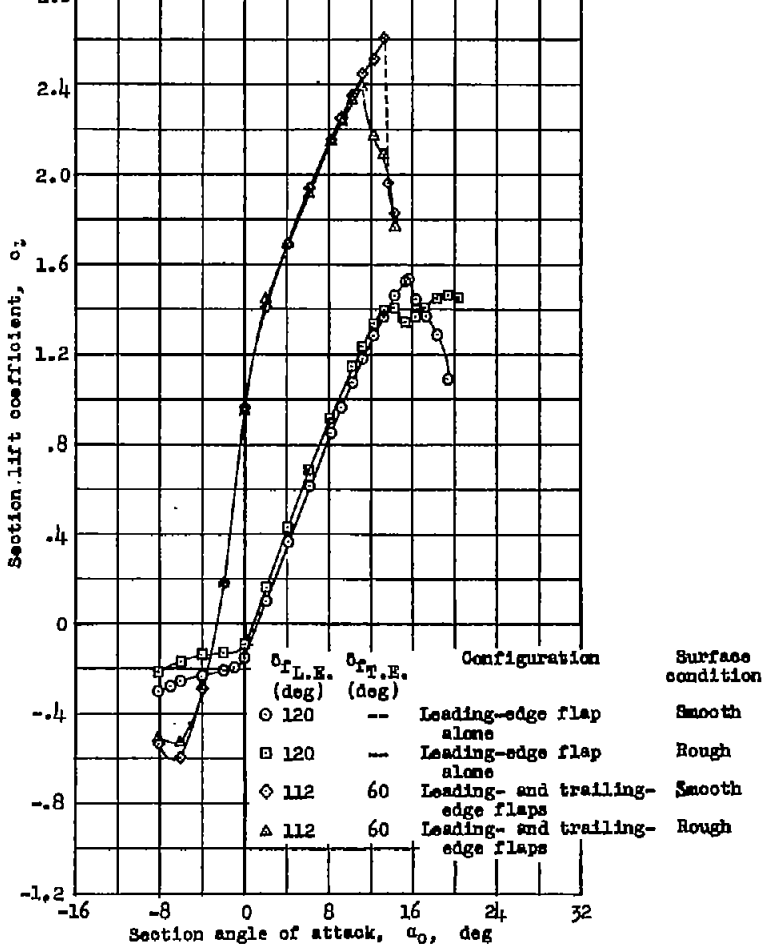

(a) Lower-surface leading-edge flap.

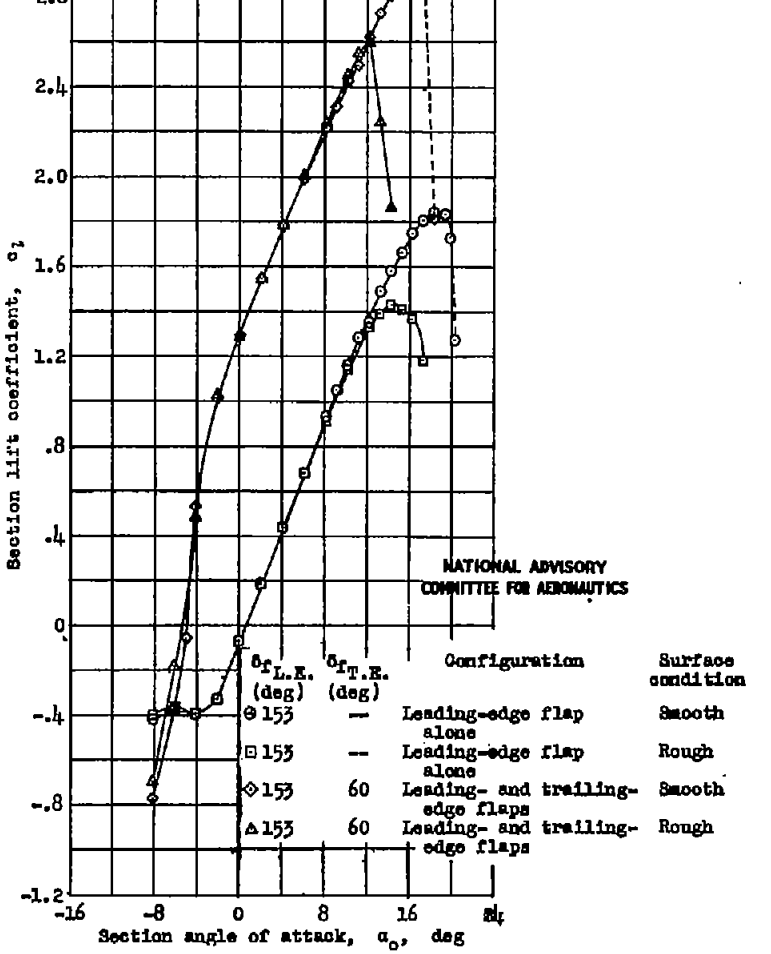

(b) Upper-surface leading-edge flap.

Figure 10.- The effect of leading-edge roughness on the section lift characteristics of the NACA 6_{4_1}-012 airfoil equipped with leading-edge and trailing-edge split flaps. $R = 6.0 \times 10^6$.

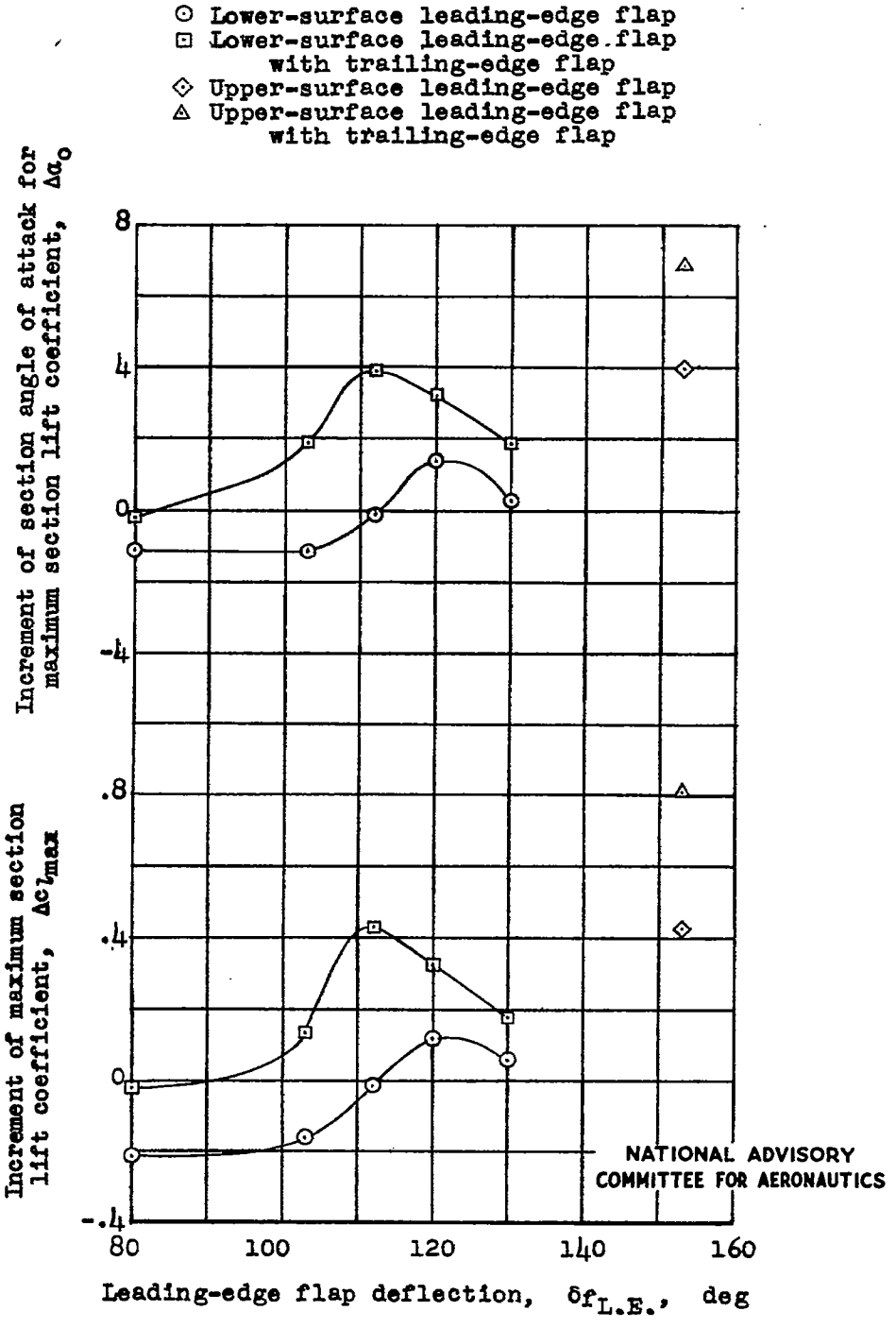

Figure 11.- Variation of the increment of maximum section lift coefficient and the increment of section angle of attack for maximum section lift coefficient with leading-edge flap deflection. NACA 64_1-012 airfoil section with leading- and trailing-edge split flaps. $R = 6.0 \times 10^6$.